Jun Chai, Bo Tian*, Yu-Feng Wang, Wen-Rong Sun and Yun-Po Wang

Conservation Laws and Mixed-Type Vector Solitons for the 3-Coupled Variable-Coefficient Nonlinear Schrödinger Equations in Inhomogeneous Multicomponent Optical Fibre

DOI 10.1515/zna-2016-0019
Received January 18, 2016; accepted March 18, 2016; previously published online April 22, 2016

Abstract: In this article, the propagation and collision of vector solitons are investigated from the 3-coupled variable-coefficient nonlinear Schrödinger equations, which describe the amplification or attenuation of the picosecond pulses in the inhomogeneous multicomponent optical fibre with different frequencies or polarizations. On the basis of the Lax pair, infinitely-many conservation laws are obtained. Under an integrability constraint among the variable coefficients for the group velocity dispersion (GVD), nonlinearity and fibre gain/loss, and two mixed-type (2-bright-1-dark and 1-bright-2-dark) vector one- and two-soliton solutions are derived via the Hirota method and symbolic computation. Influence of the variable coefficients for the GVD and nonlinearity on the vector soliton amplitudes and velocities is analysed. Through the asymptotic and graphic analysis, bound states and elastic and inelastic collisions between the vector two solitons are investigated: Not only the elastic but also inelastic collision between the 2-bright-1-dark vector two solitons can occur, whereas the collision between the 1-bright-2-dark vector two solitons is always elastic; for the bound states, the GVD and nonlinearity affect their types; with the GVD and nonlinearity being the constants, collision period decreases as the GVD increases but is independent of the nonlinearity.

Keywords: 3-Coupled Variable-Coefficient Nonlinear Schrödinger Equations; Infinitely-Many Conservation Laws; Mixed-Type Vector Soliton; Multicomponent Optical Fibre.

***Corresponding author: Bo Tian,** State Key Laboratory of Information Photonics and Optical Communications, and School of Science, Beijing University of Posts and Telecommunications, Beijing 100876, China, E-mail: tian_bupt@163.com
Jun Chai, Yu-Feng Wang, Wen-Rong Sun and Yun-Po Wang: State Key Laboratory of Information Photonics and Optical Communications, and School of Science, Beijing University of Posts and Telecommunications, Beijing 100876, China

1 Introduction

Optical solitons, formed via the balance between the group velocity dispersion (GVD) and nonlinearity [1–4], have been the subject of theoretical and experimental studies in the optical-fibre communications, due to the capability of propagating over the long distances without any change of shape and with the negligible attenuation [5–8]. Propagation of the optical solitons in the single-component fibres can be described by some nonlinear Schrödiger (NLS)-type equations [9, 10]. With the consideration on the collisions of those field components with the different frequencies or polarizations in such optical media as the multimode fibres, fibre arrays and birefringent fibres, the coupled NLS equations (e.g. the two-, three-, and N-coupled ones) have been used to describe the propagation of the vector solitons [11]. Compared with the scalar soliton which has only one polarization component, a vector soliton has the multiple distinct polarization components coupled together during the propagation [12, 13]. One phenomenon associated with the collisions of the vector solitons is the energy exchange among the components [14]. So far, three types of the vector solitons have been proposed including the bright vector solitons (all of the polarization states are the bright solitons), dark vector solitons (all dark), and mixed-type vector solitons (some bright while the others dark) [15–17]. Propagation of the vector solitons can be described by a system of the coupled NLS equations [9, 18].

Investigation on the coupled NLS equations with constant coefficients as the models of some physical problems has been performed [19–22]. Propagation of optical solitons in the inhomogeneous optical fibres can be modelled by the variable-coefficient NLS equations [5, 23–26]. Moreover, some studies on the coupled variable-coefficient NLS

equations have been presented [5, 26–32]. In this article, we investigate the propagation and collision of vector optical solitons from the 3-coupled variable-coefficient NLS equations [5],

$$iq_{1,z}+\frac{1}{2}\beta(z)q_{1,tt}+\gamma(z)\left(\sum_{n=1}^{3}|q_n|^2\right)q_1+i\delta(z)q_1=0, \tag{1a}$$

$$iq_{2,z}+\frac{1}{2}\beta(z)q_{2,tt}+\gamma(z)\left(\sum_{n=1}^{3}|q_n|^2\right)q_2+i\delta(z)q_2=0, \tag{1b}$$

$$iq_{3,z}+\frac{1}{2}\beta(z)q_{3,tt}+\gamma(z)\left(\sum_{n=1}^{3}|q_n|^2\right)q_3+i\delta(z)q_3=0, \tag{1c}$$

which have been considered as a model to describe the amplification or attenuation of the picosecond pulse propagation in the inhomogeneous multicomponent optical fibre with different frequencies or polarizations, where q_j is the complex amplitude of the j-th-field component ($j=1$, 2, 3), the subscripts z and t, respectively, represent the partial derivatives with respect to the normalised distance along the direction of the propagation and retarded time, $\beta(z)$, $\gamma(z)$, and $\delta(z)$ are the GVD, nonlinearity, and fibre gain/loss coefficients, respectively [5]. Hereby, the effect of the GVD, which can broaden a soliton, can be counterbalanced by the action of nonlinearity [11]. Therefore, it has been claimed that the soliton can use the nonlinearity to maintain its width in the presence of the GVD [11]. However, the property holds only if the fibre gain/loss is negligible, as the fibre gain/loss can lead to the change of the soliton energy [11]. Lax integrability for (1) has been confirmed under the constraint [5]

$$\delta(z)=\frac{\gamma'(z)\beta(z)-\gamma(z)\beta'(z)}{2\gamma(z)\beta(z)} \quad \text{or} \quad \delta(z)=\left[\ln\sqrt{\frac{\gamma(z)}{\beta(z)}}\right]', \tag{2}$$

where "′" means the derivative with respect to z. Darboux transformation has also been derived [5].

However, characteristics for (1), such as the infinitely-many conservation laws, bilinear forms, and mixed-type vector soliton solutions, have not yet been investigated. In Section 2, the infinitely-many conservation laws will be obtained. In Section 3, with the Hirota method [33, 34] and symbolic computation [35–37], bilinear forms and analytic mixed-type (2-bright-1-dark and 1-bright-2-dark) vector one- and two-soliton solutions for (1) will be given. Influence of the variable coefficients (GVD and nonlinearity) in (1) on the vector soliton amplitudes, velocities, and the vector soliton collisions will be analysed in Section 4. Section 5 will be our conclusions.

2 Conservation Laws

Conservation laws, which describe the conservation of physical quantities for a nonlinear evolution equation (NLEE) [38, 39], are the integrable characteristic for the NLEE. Hereby, on the basis of the Lax pair given in [5], we will construct the infinitely-many conservation laws for (1).

The corresponding Lax pair can be expressed as [5]

$$\Psi_t=U\Psi, \quad \Psi_z=V\Psi, \tag{3}$$

where the vector eigenfunction $\Psi=(\Psi_0, \Psi_1, \Psi_2, \Psi_3)^T$, T denotes the transpose of the vector, the components Ψ_0, Ψ_1, Ψ_2, and Ψ_3 are the complex functions of z and t, and U and V are expressible in the forms of

$$U=\begin{pmatrix} -i\lambda & \sqrt{\frac{\gamma(z)}{2\beta(z)}}q_1 & \sqrt{\frac{\gamma(z)}{2\beta(z)}}q_2 & \sqrt{\frac{\gamma(z)}{2\beta(z)}}q_3 \\ -\sqrt{\frac{\gamma(z)}{2\beta(z)}}q_1^* & i\lambda & 0 & 0 \\ -\sqrt{\frac{\gamma(z)}{2\beta(z)}}q_2^* & 0 & i\lambda & 0 \\ -\sqrt{\frac{\gamma(z)}{2\beta(z)}}q_3^* & 0 & 0 & i\lambda \end{pmatrix},$$

$$V=\begin{pmatrix} -2i\lambda^2 & \sqrt{\frac{\gamma(z)}{2\beta(z)}}q_1\lambda & \sqrt{\frac{\gamma(z)}{2\beta(z)}}q_2\lambda & \sqrt{\frac{\gamma(z)}{2\beta(z)}}q_3\lambda \\ -\sqrt{\frac{\gamma(z)}{2\beta(z)}}q_1^*\lambda & 2i\lambda^2 & 0 & 0 \\ -\sqrt{\frac{\gamma(z)}{2\beta(z)}}q_2^*\lambda & 0 & 2i\lambda^2 & 0 \\ -\sqrt{\frac{\gamma(z)}{2\beta(z)}}q_3^*\lambda & 0 & 0 & 2i\lambda^2 \end{pmatrix}$$

$$+\frac{i}{2}\begin{pmatrix} \gamma(z)\sum_{j=1}^{3}|q_j|^2 & \sqrt{2\gamma(z)\beta(z)}q_{1t} & \sqrt{2\gamma(z)\beta(z)}q_{2t} & \sqrt{2\gamma(z)\beta(z)}q_{3t} \\ \sqrt{2\gamma(z)\beta(z)}(q_1^*)_t & -\gamma(z)|q_1|^2 & -\gamma(z)q_2q_1^* & -\gamma(z)q_3q_1^* \\ \sqrt{2\gamma(z)\beta(z)}(q_2^*)_t & -\gamma(z)q_1q_2^* & -\gamma(z)|q_2|^2 & -\gamma(z)q_3q_2^* \\ \sqrt{2\gamma(z)\beta(z)}(q_3^*)_t & -\gamma(z)q_1q_3^* & -\gamma(z)q_2q_3^* & -\gamma(z)|q_3|^2 \end{pmatrix},$$

with λ as the spectral parameter.

Introducing the functions $\Gamma_j=\frac{\Psi_j}{\Psi_0}$ $(j=1, 2, 3)$, we get the following Ricatti equations:

$$\Gamma_{j,t}=-\varrho q_j^*+2i\lambda\Gamma_j-\sum_{l=1}^{3}(\varrho q_l\Gamma_l)\Gamma_j, \tag{4}$$

with $\varrho=\sqrt{\frac{\gamma(z)}{2\beta(z)}}$.

We expand $\varrho q_j\Gamma_j$ as a power series of λ^{-1}, namely,

$$\varrho q_j\Gamma_j=\sum_{n=1}^{\infty}F_n^{(j)}\lambda^{-n}, \tag{5}$$

where $F_n^{(j)}$'s $(n=1, 2, \ldots)$ are the functions of z and t to be determined.

Then, substituting Expression (5) into Expression (4) and equating the coefficients of the same power of λ to zero, we can obtain the recurrence relations,

$$F_1^{(j)}=\frac{1}{2i}\varrho^2|q_j|^2, \tag{6a}$$

$$F_2^{(j)}=\frac{1}{2i}\left\{\frac{-q_{jt}}{q_j}F_1^{(j)}+F_{1,t}^{(j)}\right\}, \tag{6b}$$

$$F_{r+1}^{(j)}=\frac{1}{2i}\left\{\frac{-q_{jt}}{q_j}F_r^{(j)}+\sum_{l=1}^{r-1}\left[\sum_{s=1}^{3}F_l^{(s)}\right]F_{r-l}^{(j)}+F_{r,t}^{(j)}\right\},\ (r=2, 3, 4\ldots). \tag{6c}$$

Through the compatibility condition $(\ln\Psi_0)_{tz}=(\ln\Psi_0)_{zt}$, we can obtain the following conservation form:

$$[-i\lambda+\varrho q_1\Gamma_1+\varrho q_2\Gamma_2+\varrho q_3\Gamma_3]_z=[Q_0+Q_1\Gamma_1+Q_2\Gamma_2+Q_3\Gamma_3]_t, \tag{7}$$

with

$$Q_0=-2i\lambda^2+\frac{i}{2}\gamma(z)\sum_{j=1}^{3}|q_j|^2,$$

$$Q_1=\varrho q_1\lambda+\frac{i}{2}\sqrt{2\gamma(z)\beta(z)}q_{1t},$$

$$Q_2=\varrho q_2\lambda+\frac{i}{2}\sqrt{2\gamma(z)\beta(z)}q_{2t},$$

$$Q_3=\varrho q_3\lambda+\frac{i}{2}\sqrt{2\gamma(z)\beta(z)}q_{3t}.$$

Substituting Expressions (5) and (6) into Expression (7) yields the infinitely-many conservation laws,

$$\frac{\partial}{\partial z}R_n+\frac{\partial}{\partial t}J_n=0,\ n=1, 2, \ldots, \tag{8}$$

with

$$R_1=-\frac{1}{2}i\varrho^2\sum_{j=1}^{3}|q_j|^2, \tag{9}$$

$$J_1=\frac{1}{4}\varrho^2\sum_{j=1}^{3}[q_j(q_j^*)_t]-\frac{1}{4}\gamma(z)\sum_{j=1}^{3}(q_j^*q_{jt}), \tag{10}$$

$$R_2=-\frac{1}{4}\varrho^2\sum_{j=1}^{3}[q_j(q_j^*)_t], \tag{11}$$

$$J_2=-\frac{i}{8}\varrho^4\sum_{j=1}^{3}|q_j|^4-\frac{i}{4}\varrho^4\sum_{j,l=1,j\neq l}^{3}(|q_j|^2|q_l|^2)+\frac{i}{8}\gamma(z)\sum_{j=1}^{3}[q_{jt}(q_j^*)_t]$$
$$-\frac{i}{8}\varrho^2\sum_{j=1}^{3}[q_j(q_j^*)_{tt}], \tag{12}$$

$$R_3=\frac{1}{8}i\varrho^2\left\{\varrho^2\sum_{j=1}^{3}|q_j|^4+2\varrho^2\sum_{j,l=1,j\neq l}^{3}(|q_j|^2|q_l|^2)+\sum_{j=1}^{3}[q_j(q_j^*)_{tt}]\right\}, \tag{13}$$

$$J_3=\frac{1}{16}\gamma(z)\varrho^2\sum_{j,l=1}^{3}(|q_l|^2q_j^*q_{jt})+\frac{1}{16}\gamma(z)\sum_{j=1}^{3}[q_{jt}(q_j^*)_{tt}], \tag{14}$$

$\vdots$

where R_n's and J_n's represent the conserved densities and conserved fluxes, respectively.

3 Bilinear Forms and Vector Soliton Solutions for (1)

3.1 Bilinear Forms

Under Constraint (2), introducing the following dependent variable transformations [23]:

$$q_j=\sqrt{\frac{\beta(z)}{\gamma(z)}}\frac{g^{(j)}}{f},\ (j=1, 2, 3), \tag{15}$$

where $g^{(j)}$'s are all the complex functions to be determined and f is a real one, we can transform (1) into the bilinear forms

$$\left[iD_z+\frac{\beta(z)}{2}D_t^2-\zeta(z)\right]g^{(j)}\cdot f=0, \tag{16a}$$

$$\left[\frac{\beta(z)}{2}D_t^2-\zeta(z)\right]f\cdot f=\beta(z)\sum_{j=1}^{3}|g^{(j)}|^2, \tag{16b}$$

where $\zeta(z)$ is a real function to be determined, and the bilinear operators D_z and D_t are defined by [33, 34]:

$$D_z^{m_1}D_t^{m_2}(G\cdot F)=\left(\frac{\partial}{\partial z}-\frac{\partial}{\partial z'}\right)^{m_1}\left(\frac{\partial}{\partial t}-\frac{\partial}{\partial t'}\right)^{m_2}G(z,t)F(z',t')|_{z'=z,t'=t},$$

with $G(z, t)$ as a differentiable function of z and t, $F(z', t')$ as a differentiable function of the formal variables z' and t', m_1, and m_2 as two non-negative integers.

3.2 Vector Soliton Solutions

3.2.1 2-Bright-1-Dark Vector Soliton Solutions

In order to obtain the 2-bright-1-dark vector soliton solutions for (1), we expand $g^{(j)}$ ($j=1, 2, 3$) and f with respect to a formal expansion parameter ε as follows:

$$g^{(j)}=\varepsilon g_1^{(j)}+\varepsilon^3 g_3^{(j)}+\varepsilon^5 g_5^{(j)}+\cdots,\ (j=1,\ 2), \tag{17a}$$

$$g^{(3)}=g_0^{(3)}[1+\varepsilon^2 g_2^{(3)}+\varepsilon^4 g_4^{(3)}+\varepsilon^6 g_6^{(3)}+\cdots], \tag{17b}$$

$$f=1+\varepsilon^2 f_2+\varepsilon^4 f_4+\varepsilon^6 f_6+\cdots, \tag{17c}$$

where $g_O^{(j)}$'s ($O=1, 3, 5, \ldots$) and $g_L^{(3)}$'s ($L=0, 2, 4, 6, \ldots$) are all the complex functions to be determined, f_W's ($W=2, 4, 6, \ldots$) are the real functions to be determined.

(A) 2-bright-1-dark vector one-soliton solutions

Truncating Expression (17) as $g^{(j)}=\varepsilon g_1^{(j)}$ ($j=1, 2$), $g^{(3)}=g_0^{(3)}[1+\varepsilon^2 g_2^{(3)}]$ and $f=1+\varepsilon^2 f_2$, and substituting them into Bilinear Forms (16), we obtain the 2-bright-1-dark vector one-soliton solutions for (1) as

$$q_j=\sqrt{\frac{\beta(z)}{\gamma(z)}}\frac{g_1^{(j)}}{1+f_2},\ (j=1,\ 2), \tag{18a}$$

$$q_3=\sqrt{\frac{\beta(z)}{\gamma(z)}}\frac{g_0^{(3)}[1+g_2^{(3)}]}{1+f_2}, \tag{18b}$$

where

$$g_1^{(j)}=a^{(j)}e^{\theta},\ g_0^{(3)}=\chi e^{\phi},\ g_2^{(3)}=\kappa e^{\theta+\theta^*},\ f_2=\tau e^{\theta+\theta^*},\ \zeta(z)=-\chi\chi^*\beta(z),$$

$$\phi=ipt+\frac{i}{2}\int[(2\chi\chi^*-p^2)\beta(z)]\mathrm{d}z,\ \theta=\eta t+\frac{i}{2}\int[(2\chi\chi^*+\eta^2)\beta(z)]\mathrm{d}z,$$

$$\kappa=\frac{(p+i\eta)\tau}{p-i\eta^*},\ \tau=\frac{[a^{(1)}+a^{(1)*}+a^{(2)}+a^{(2)*}](p+i\eta)(p-i\eta^*)}{(\eta+\eta^*)^2[\chi\chi^*+(p+i\eta)(p-i\eta^*)]},$$

with $*$ as the complex conjugate, $a^{(j)}$'s, χ, η, and p as all the constants.

(B) 2-bright-1-dark vector two-soliton solutions

To derive the 2-bright-1-dark vector two-soliton solutions for (1), we truncate Expression (17) as $g^{(j)}=\varepsilon g_1^{(j)}+\varepsilon^3 g_1^{(j)}$ ($j=1, 2$), $g^{(3)}=g_0^{(3)}[1+\varepsilon^2 g_2^{(3)}+\varepsilon^4 g_4^{(3)}]$ and $f=1+\varepsilon^2 f_2+\varepsilon^4 f_4$, and substitute them into Bilinear Forms (16). Then we get

$$q_j=\sqrt{\frac{\beta(z)}{\gamma(z)}}\frac{g_1^{(j)}+g_3^{(j)}}{1+f_2+f_4},\ (j=1,\ 2), \tag{19a}$$

$$q_3=\sqrt{\frac{\beta(z)}{\gamma(z)}}\frac{g_0^{(3)}[1+g_2^{(3)}+g_4^{(3)}]}{1+f_2+f_4}, \tag{19b}$$

where

$$g_1^{(j)}=a_1^{(j)}e^{\theta_1}+a_2^{(j)}e^{\theta_2},\ g_3^{(j)}=A_1^{(j)}e^{\theta_1+\theta_2+\theta_1^*}+A_2^{(j)}e^{\theta_1+\theta_2+\theta_2^*},\ g_0^{(3)}=\chi e^{\phi},$$

$$g_2^{(3)}=\kappa_1 e^{\theta_1+\theta_1^*}+\kappa_2 e^{\theta_2+\theta_1^*}+\kappa_3 e^{\theta_1+\theta_2^*}+\kappa_4 e^{\theta_2+\theta_2^*},\ g_4^{(3)}=\rho e^{\theta_1+\theta_1^*+\theta_2+\theta_2^*},$$

$$f_2=\tau_1 e^{\theta_1+\theta_1^*}+\tau_2 e^{\theta_2+\theta_1^*}+\tau_3 e^{\theta_1+\theta_2^*}+\tau_4 e^{\theta_2+\theta_2^*},\ f_4=he^{\theta_1+\theta_1^*+\theta_2+\theta_2^*},$$

$$\theta_1=\eta_1 t+\frac{i}{2}\int[(2\chi\chi^*+\eta_1^2)\beta(z)]\mathrm{d}z,\ \theta_2=\eta_2 t+\frac{i}{2}\int[(2\chi\chi^*+\eta_2^2)\beta(z)]\mathrm{d}z,$$

$$\phi=ipt+\frac{i}{2}\int[(2\chi\chi^*-p^2)\beta(z)]\mathrm{d}z,\ \zeta(z)=-\chi\chi^*\beta(z),$$

$$A_1^{(j)}=(\eta_1-\eta_2)\left[\frac{a_1^{(j)}\tau_2}{\eta_1+\eta_1^*}-\frac{a_2^{(j)}\tau_1}{\eta_2+\eta_1^*}\right],\ A_2^{(j)}=(\eta_1-\eta_2)\left[\frac{a_1^{(j)}\tau_4}{\eta_1+\eta_2^*}-\frac{a_2^{(j)}\tau_3}{\eta_2+\eta_2^*}\right],$$

$$\kappa_1=\frac{(p+i\eta_1)\tau_1}{p-i\eta_1^*},\ \kappa_2=\frac{(p+i\eta_2)\tau_2}{p-i\eta_1^*},\ \kappa_3=\frac{(p+i\eta_1)\tau_3}{p-i\eta_2^*},\ \kappa_4=\frac{(p+i\eta_2)\tau_4}{p-i\eta_2^*},$$

$$\tau_1=\frac{[a_1^{(1)}a_1^{(1)*}+a_1^{(2)}a_1^{(2)*}](p+i\eta_1)(p-i\eta_1^*)}{(\eta_1+\eta_1^*)^2[(p+i\eta_1)(p-i\eta_1^*)+\chi\chi^*]},$$

$$\tau_2=\frac{[a_2^{(1)}a_1^{(1)*}+a_2^{(2)}a_1^{(2)*}](p+i\eta_2)(p-i\eta_1^*)}{(\eta_2+\eta_1^*)^2[(p+i\eta_2)(p-i\eta_1^*)+\chi\chi^*]},$$

$$\tau_3=\frac{[a_1^{(1)}a_2^{(1)*}+a_1^{(2)}a_1^{(2)*}](p+i\eta_1)(p-i\eta_2^*)}{(\eta_1+\eta_2^*)^2[(p+i\eta_1)(p-i\eta_2^*)+\chi\chi^*]},$$

$$\tau_4=\frac{[a_2^{(1)}a_2^{(1)*}+a_2^{(2)}a_2^{(2)*}](p+i\eta_2)(p-i\eta_2^*)}{(\eta_2+\eta_2^*)^2[(p+i\eta_2)(p-i\eta_2^*)+\chi\chi^*]},$$

$$\rho=\frac{h(p+i\eta_1)(p+i\eta_2)}{(p-i\eta_1^*)(p-i\eta_2^*)},\ h=\frac{\tau_1\tau_4(\eta_1-\eta_2)(\eta_1^*-\eta_2^*)}{(\eta_1+\eta_2^*)(\eta_2+\eta_1^*)}$$

$$-\frac{\tau_2\tau_3(\eta_1-\eta_2)(\eta_1^*-\eta_2^*)}{(\eta_1+\eta_1^*)(\eta_2+\eta_2^*)},$$

with $a_1^{(j)}$'s, $a_2^{(j)}$'s, χ, η_1, η_2, and p as all the constants.

3.2.2 1-Bright-2-Dark Vector Soliton Solutions

Similarly, we take

$$g^{(1)}=\varepsilon g_1^{(1)}+\varepsilon^3 g_3^{(1)}+\varepsilon^5 g_5^{(1)}+\cdots, \tag{20a}$$

$$g^{(j)}=g_0^{(j)}[1+\varepsilon^2 g_2^{(j)}+\varepsilon^4 g_4^{(j)}+\varepsilon^6 g_6^{(j)}+\cdots],\ (j=2,\ 3) \tag{20b}$$

$$f=1+\varepsilon^2 f_2+\varepsilon^4 f_4+\varepsilon^6 f_6+\cdots, \tag{20c}$$

where $g_l^{(1)}$'s ($l=1, 3, 5, \ldots$) and $g_b^{(j)}$'s ($b=0, 2, 4, 6, \ldots$) are all the complex functions to be determined, f_w's ($w=2, 4, 6, \ldots$) are the real functions to be determined.

(A) 1-bright-2-dark vector one-soliton solutions

We truncate Expression (20) as $g^{(1)}=\varepsilon g_1^{(1)}$, $g^{(j)}=g_0^{(j)}[1+\varepsilon^2 g_2^{(j)}]$ ($j=2, 3$), $f=1+\varepsilon^2 f_2$, substitute them into Bilinear Forms (16), and obtain

$$q_1=\sqrt{\frac{\beta(z)}{\gamma(z)}}\frac{g_1^{(1)}}{1+f_2}, \tag{21a}$$

$$q_j=\sqrt{\frac{\beta(z)}{\gamma(z)}}\frac{g_0^{(j)}[1+g_2^{(j)}]}{1+f_2},\ (j=2, 3), \tag{21b}$$

where

$$g^{(1)}=ae^{\Theta}, g_0^{(j)}=\chi_j e^{\phi_j}, g_2^{(j)}=\tau_j e^{\Theta+\Theta^*}, f_2=\kappa e^{\Theta+\Theta^*},$$

$$\phi_j=ip_j t+i\int\left[\left(-\frac{1}{2}p_j^2+\chi_2\chi_2^*+\chi_3\chi_3^*\right)\beta(z)\right]\mathrm{d}z,$$

$$\Theta=\mu t+i\int\left[\left(-\frac{1}{2}\mu^2+\chi_2\chi_2^*+\chi_3\chi_3^*\right)\beta(z)\right]\mathrm{d}z,$$

$$\lambda(z)=-\chi_2\chi_2^*\beta(z)-\chi_3\chi_3^*\beta(z), \tau_j=\frac{\kappa(p_j+i\mu)}{(p_j-i\mu^*)},$$

$$\kappa=\frac{aa^*H}{(\mu+\mu^*)^2[H+(p_3+i\mu)(p_3-i\mu^*)\chi_2\chi_2^*+(p_2+i\mu)(p_2-i\mu^*)\chi_3\chi_3^*]},$$

$$H=(p_2+i\mu)(p_2-i\mu^*)(p_3+i\mu)(p_3-i\mu^*),$$

with a, χ_j's, μ, and p_j's as all the constants.

(B) 1-bright-2-dark vector two-soliton solutions

With the truncations of Expression (20) $g^{(1)}=\varepsilon g_1^{(1)}+\varepsilon^3 g_3^{(1)}$, $g^{(j)}=g_0^{(j)}[1+\varepsilon^2 g_2^{(j)}+\varepsilon^4 g_4^{(j)}]$ ($j=2, 3$) and $f=1+\varepsilon^2 f_2+\varepsilon^4 f_4$, we get the vector two-soliton solutions for (1),

$$q_1=\sqrt{\frac{\beta(z)}{\gamma(z)}}\frac{g_1^{(1)}+g_3^{(1)}}{1+f_2+f_4}, \tag{22a}$$

$$q_j=\sqrt{\frac{\beta(z)}{\gamma(z)}}\frac{g_0^{(j)}[1+g_2^{(j)}+g_4^{(j)}]}{1+f_2+f_4},\ (j=2, 3), \tag{22b}$$

where

$$g_1^{(1)}=a_1e^{\Theta_1}+a_2e^{\Theta_2}, g_3^{(1)}=A_1e^{\Theta_1+\Theta_2+\Theta_1^*}+A_2e^{\Theta_1+\Theta_2+\Theta_2^*}, g_0^{(j)}=\chi_j e^{\phi_j},$$

$$g_2^{(j)}=\kappa_1^{(j)}e^{\Theta_1+\Theta_1^*}+\kappa_2^{(j)}e^{\Theta_2+\Theta_1^*}+\kappa_3^{(j)}e^{\Theta_1+\Theta_2^*}+\kappa_4^{(j)}e^{\Theta_2+\Theta_2^*},$$

$$g_4^{(j)}=\varsigma^{(j)}e^{\Theta_1+\Theta_2+\Theta_1^*+\Theta_2^*}, f_2=\sigma_1e^{\Theta_1+\Theta_1^*}+\sigma_2e^{\Theta_2+\Theta_1^*}+\sigma_3e^{\Theta_1+\Theta_2^*}$$
$$+\sigma_4e^{\Theta_2+\Theta_2^*}, f_4=\nu e^{\Theta_1+\Theta_2+\Theta_1^*+\Theta_2^*}, \lambda(z)=-\chi_2\chi_2^*\beta(z)-\chi_3\chi_3^*\beta(z),$$

$$\phi_j=ip_jt+i\int\left[\left(-\frac{1}{2}p_j^2+\chi_2\chi_2^*+\chi_3\chi_3^*\right)\beta(z)\right]\mathrm{d}z,$$

$$\Theta_1=\mu_1t+i\int\left[\left(-\frac{1}{2}\mu_1^2+\chi_2\chi_2^*+\chi_3\chi_3^*\right)\beta(z)\right]\mathrm{d}z,$$

$$\Theta_2=\mu_2t+i\int\left[\left(-\frac{1}{2}\mu_2^2+\chi_2\chi_2^*+\chi_3\chi_3^*\right)\beta(z)\right]\mathrm{d}z,$$

$$\kappa_1^{(j)}=\frac{(p_j+i\mu_1)\sigma_1}{p_j-i\mu_1^*}, \kappa_2^{(j)}=\frac{(p_j+i\mu_2)\sigma_2}{p_j-i\mu_1^*},$$

$$\kappa_3^{(j)}=\frac{(p_j+i\mu_1)\sigma_3}{p_j-i\mu_2^*}, \kappa_4^{(j)}=\frac{(p_j+i\mu_2)\sigma_4}{p_j-i\mu_2^*},$$

$$\sigma_1=\frac{a_1a_1^*H_1}{(\mu_1+\mu_1^*)^2[H_1+(p_3+i\mu_1)(p_3-i\mu_1^*)\chi_2\chi_2^*+(p_2+i\mu_1)(p_2-i\mu_1^*)\chi_3\chi_3^*]},$$

$$\sigma_2=\frac{a_2a_1^*H_2}{(\mu_2+\mu_1^*)^2[H_2+(p_3+i\mu_2)(p_3-i\mu_1^*)\chi_2\chi_2^*+(p_2+i\mu_2)(p_2-i\mu_1^*)\chi_3\chi_3^*]},$$

$$\sigma_3=\frac{a_1a_2^*H_3}{(\mu_1+\mu_2^*)^2[H_3+(p_3+i\mu_1)(p_3-i\mu_2^*)\chi_2\chi_2^*+(p_2+i\mu_1)(p_2-i\mu_2^*)\chi_3\chi_3^*]},$$

$$\sigma_4=\frac{a_2a_2^*H_4}{(\mu_2+\mu_2^*)^2[H_4+(p_3+i\mu_2)(p_3-i\mu_2^*)\chi_2\chi_2^*+(p_2+i\mu_2)(p_2-i\mu_2^*)\chi_3\chi_3^*]},$$

$$H_1=(p_2+i\mu_1)(p_2-i\mu_1^*)(p_3+i\mu_1)(p_3-i\mu_1^*),$$

$$H_2=(p_2+i\mu_2)(p_2-i\mu_1^*)(p_3+i\mu_2)(p_3-i\mu_1^*),$$

$$H_3=(p_2+i\mu_1)(p_2-i\mu_2^*)(p_3+i\mu_1)(p_3-i\mu_2^*),$$

$$H_4=(p_2+i\mu_2)(p_2-i\mu_2^*)(p_3+i\mu_2)(p_3-i\mu_2^*),$$

$$A_1=-\frac{(\eta_1-\eta_2)[a_2\sigma_1(\eta_1+\eta_1^*)-a_1\sigma_3(\eta_1^*+\eta_2)]}{(\eta_1+\eta_1^*)(\eta_2+\eta_1^*)},$$

$$A_2=-\frac{(\eta_1-\eta_2)[a_2\sigma_2(\eta_1+\eta_2^*)-a_1\sigma_4(\eta_2^*+\eta_2)]}{(\eta_1+\eta_2^*)(\eta_2+\eta_2^*)},$$

$$\varsigma^{(j)}=\frac{\nu(p_j+i\mu_1)(p_j+i\mu_2)}{(p_j-i\mu_1^*)(p_j-i\mu_2^*)}, \nu=\frac{\sigma_1\sigma_4(\mu_1-\mu_2)(\mu_1^*-\mu_2^*)}{(\mu_1+\mu_2^*)(\mu_2+\mu_1^*)}$$
$$-\frac{\sigma_2\sigma_3(\mu_1-\mu_2)(\mu_1^*-\mu_2^*)}{(\mu_1+\mu_1^*)(\mu_2+\mu_2^*)},$$

with a_1, a_2, χ_j's, μ_1, μ_2, and p_j's as all the constants.

4 Discussion on the Vector Solitons

4.1 Vector One Soliton

In this section, we investigate the properties of the vector solitons based on Solutions (18) and (21), such as the velocities and amplitudes of the bright and dark solitons.

From Solutions (18), we can obtain the velocities $[v_j\,(j=1,\,2,\,3)]$ and amplitudes $[\Delta_j\,(j=1,\,2,\,3)]$ of the 2-bright-1-dark vector soliton as

$$v_j = Im(\eta)\beta(z)\ (j=1,\,2,\,3), \tag{23a}$$

$$\Delta_j = \frac{1}{2}\left|a^{(j)}\sqrt{\frac{\beta(z)}{\gamma(z)\tau}}\right|\ (j=1,\,2), \tag{23b}$$

$$\Delta_3 = \left|\chi\sqrt{\frac{\beta(z)}{\gamma(z)}}\right|, \tag{23c}$$

with *Re* and *Im* as the real part and imaginary part of the parameter, respectively.

The velocities $[\tilde{v}_j(j=1,\,2,\,3)]$ and amplitudes $[\tilde{\Delta}_j\ (j=1,\,2,\,3)]$ of the 1-bright-2-dark vector soliton via Solutions (21) are derived as

$$\tilde{v}_j = Im(\mu)\beta(z)\ (j=1,\,2,\,3), \tag{24a}$$

$$\tilde{\Delta}_1 = \frac{1}{2}\left|a\sqrt{\frac{\beta(z)}{\gamma(z)\kappa}}\right|, \tag{24b}$$

$$\tilde{\Delta}_j = \left|\chi_j\sqrt{\frac{\beta(z)}{\gamma(z)}}\right|\ (j=2,\,3). \tag{24c}$$

From Expressions (23) and (24), we find that the amplitudes of the two mixed-type vector solitons are both related to $\beta(z)$ and $\gamma(z)$, but the velocities of them are only related to $\beta(z)$.

2-Bright-1-dark vector soliton via Solutions (18) is shown in Figures 1–3, while 1-bright-2-dark vector soliton via Solutions (21) is displayed in Figures 4–6. In Figures 1, 2, 4, and 5, with $\beta(z)=\gamma(z)$ leading to $\delta(t)=0$, we find that amplitudes of the vector solitons keep unchanged during the propagation. It indicates that, with the absence of the fibre gain/loss, the vector soliton can propagate without the energy change. Besides, if we consider the homogeneous optical fibre, where $\beta(z)$ and $\gamma(z)$ both being the constants, vector solitons propagate stably with the invariable velocities, as shown in Figures 1 and 4. However, in the inhomogeneous optical fibre, choosing $\beta(z)=\gamma(z)=0.1z^2$ in Figure 2 while $\beta(z)=\gamma(z)=\cos(z)$ in Figure 5, we find that the vector soliton propagates *S*-shaped and periodically, respectively. The velocity of the vector soliton shown in Figure 2 slowly decreases and eventually approaches a steady positive velocity for $t\to+\infty$ or $-\infty$, while that shown in Figure 5 changes periodically. Amplitude-changing vector soliton can be obtained, when the value of $\frac{\beta(z)}{\gamma(z)}$ is variable, i.e. $\delta(t)\neq 0$, as shown in Figures 3 and 6. The presence of the fibre gain/loss can cause the change of the soliton energy. In addition, owing to the different choices of $\beta(z)$, the velocity of the vector soliton shown in Figure 3 gradually increases with *t*, while that of the vector soliton shown in Figure 6 keeps unchanged.

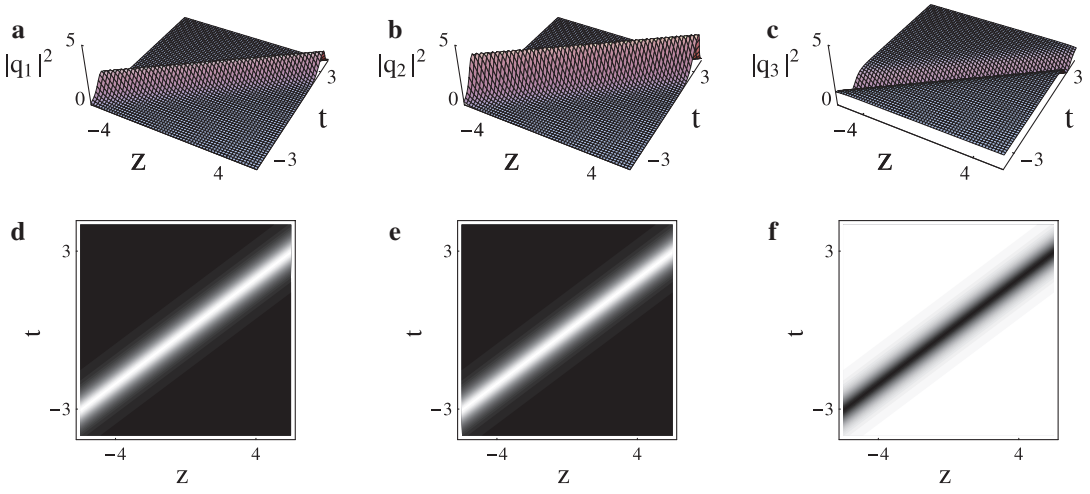

Figure 1: (a–c) Three-dimensional graphs of the 2-bright-1-dark vector one soliton via Solutions (18) with $a^{(1)}=3$, $a^{(2)}=4$, $\eta=2+i$, $\chi=1+0.5i$, $p=1$, $\beta(z)=\gamma(z)=0.5$. (d–f) Contour plots of (a–c), respectively.

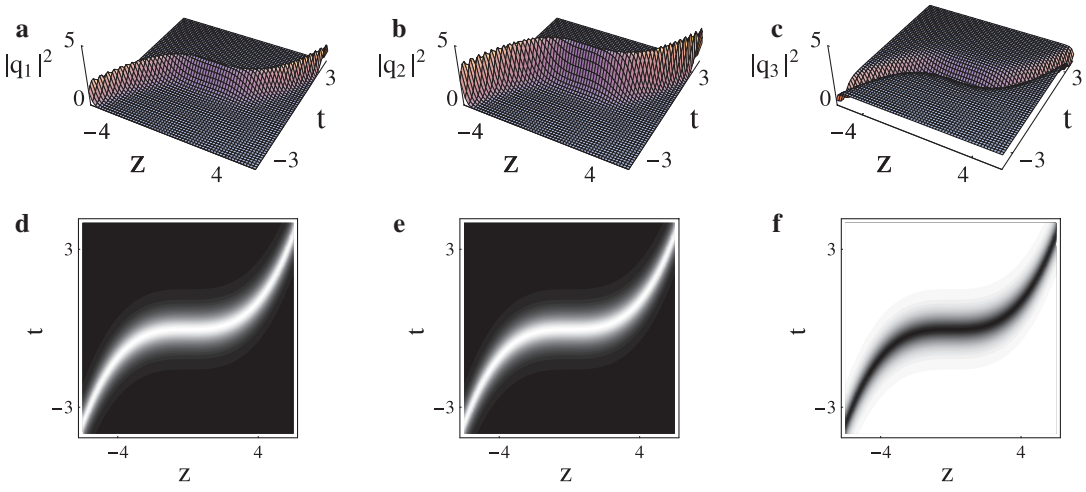

Figure 2: The same as Figure 1 except that $\beta(z)=\gamma(z)=0.1z^2$.

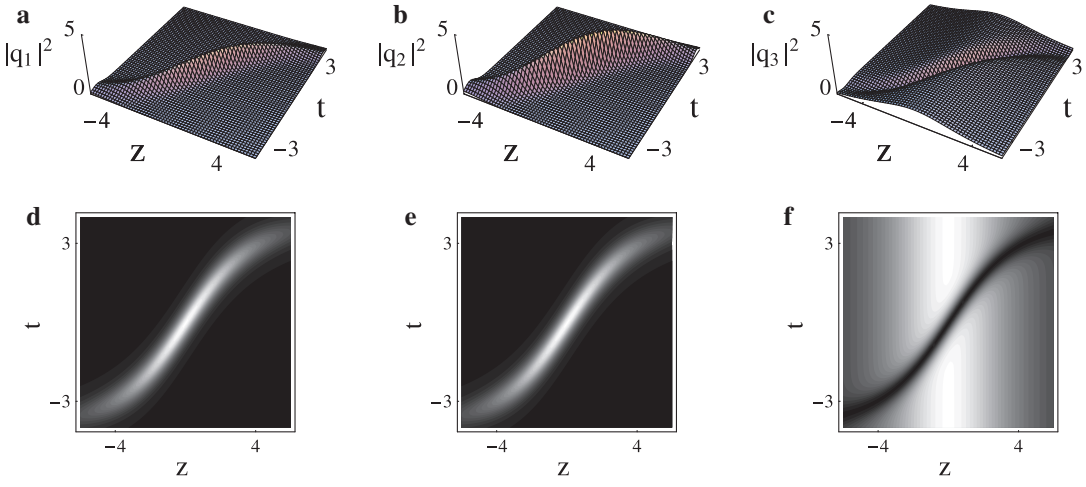

Figure 3: The same as Figure 1 except that $\beta(z)=\mathrm{sech}(0.4z)$, $\gamma(z)=1$.

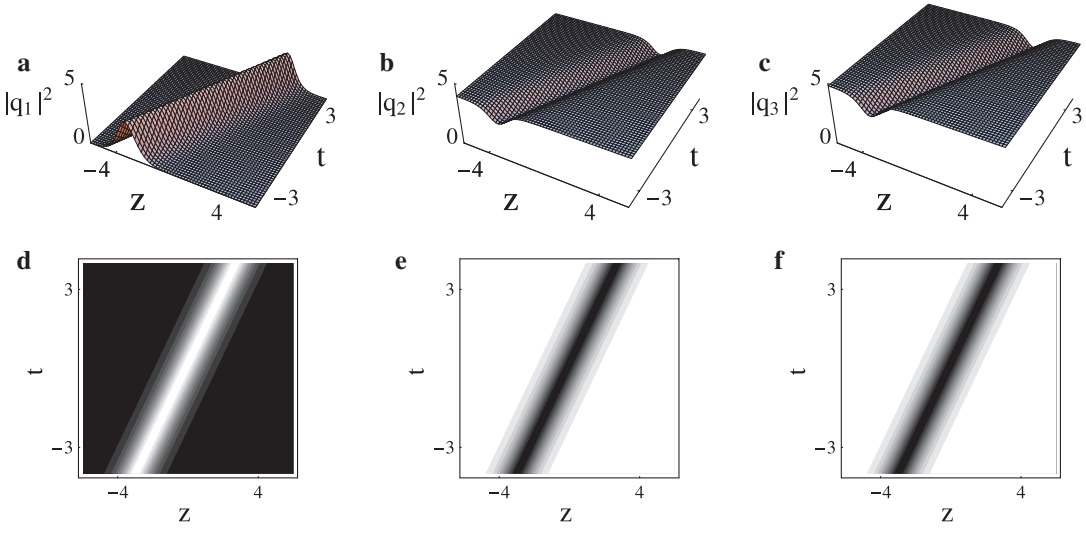

Figure 4: (a–c) Three-dimensional graphs of the 1-bright-2dark vector one soliton via Solutions (21) with $a=3$, $\chi_2=2$, $\chi_3=2.2$, $\mu=0.8+0.7i$, $p_2=p_3=2$, $\beta(z)=\gamma(z)=2$. (d–f) Contour plots of (a–c), respectively.

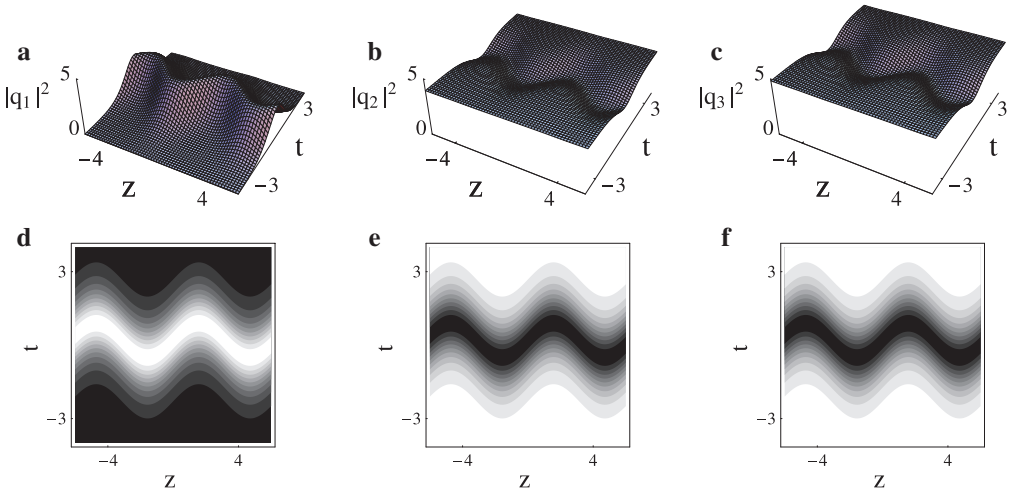

Figure 5: The same as Figure 4 except that $\beta(z)=\gamma(z)=\cos(z)$.

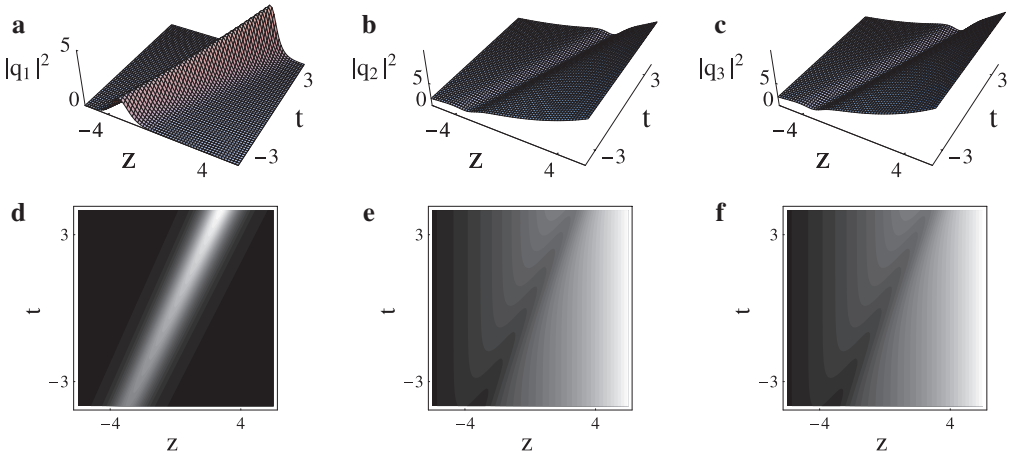

Figure 6: The same as Figure 4 except that $\beta(z)=2$, $\gamma(z)=2.5e^{-0.15z}$.

4.2 Vector Two Solitons

4.2.1 Elastic and Inelastic Collisions of the Vector Two Solitons

On the basis of Solutions (19) and (22), in this part, we will investigate the elastic and inelastic collisions of the vector solitons via the asymptotic and graphical analysis, in the case that the choices of the GVD coefficient $\beta(t)$ and nonlinearity coefficient $\gamma(t)$ lead to the fibre gain/loss coefficient $\delta(t)=0$.

(A) Asymptotic analysis on Solutions (19)

Before the collision ($z\to-\infty$),

$$q_j^{1-}\to\sqrt{\frac{\beta(z)}{\gamma(z)}}\frac{a_1^{(j)}e^{\theta_1}}{1+\tau_1 e^{\theta_1+\theta_1^*}}\ (j=1,\ 2),\ (\theta_1+\theta_1^*\sim 0,\ \theta_2+\theta_2^*\to-\infty), \tag{25a}$$

$$q_3^{1-}\to\sqrt{\frac{\beta(z)}{\gamma(z)}}\frac{\chi e^{\phi}(1+\kappa_1 e^{\theta_1+\theta_1^*})}{1+\tau_1 e^{\theta_1+\theta_1^*}},\quad (\theta_1+\theta_1^*\sim 0,\ \theta_2+\theta_2^*\to-\infty), \tag{25b}$$

$$q_j^{2-}\to\sqrt{\frac{\beta(z)}{\gamma(z)}}\frac{A_1^{(j)}e^{\theta_2}}{\tau_1+he^{\theta_2+\theta_2^*}}\ (j=1,\ 2),\ (\theta_2+\theta_2^*\sim 0,\ \theta_1+\theta_1^*\to+\infty), \tag{25c}$$

$$q_3^{2-}\to\sqrt{\frac{\beta(z)}{\gamma(z)}}\frac{\chi e^{\phi}(\kappa_1+\rho e^{\theta_2+\theta_2^*})}{\tau_1+he^{\theta_2+\theta_2^*}},\quad (\theta_2+\theta_2^*\sim 0,\ \theta_1+\theta_1^*\to+\infty), \tag{25d}$$

with q_j^{1-}'s and q_j^{2-}'s ($j=1, 2, 3$) as the asymptotic expressions for the vector two solitons before the collision, respectively.

After the collision ($z\to+\infty$),

$$q_j^{1+}\to\sqrt{\frac{\beta(z)}{\gamma(z)}}\frac{A_2^{(j)}e^{\theta_1}}{\tau_4+he^{\theta_1+\theta_1^*}}\ (j=1,\ 2),\ (\theta_1+\theta_1^*\sim 0,\ \theta_2+\theta_2^*\to+\infty), \tag{26a}$$

$$q_3^{1+}\to\sqrt{\frac{\beta(z)}{\gamma(z)}}\frac{\chi e^{\phi}(\tau_4+\rho e^{\theta_1+\theta_1^*})}{\tau_4+he^{\theta_1+\theta_1^*}},\quad (\theta_1+\theta_1^*\sim 0,\ \theta_2+\theta_2^*\to+\infty), \tag{26b}$$

$$q_j^{2+}\to\sqrt{\frac{\beta(z)}{\gamma(z)}}\frac{a_2^{(j)}e^{\theta_2}}{1+\tau_4 e^{\theta_2+\theta_2^*}}\ (j=1,\ 2),\ (\theta_2+\theta_2^*\sim 0,\ \theta_1+\theta_1^*\to-\infty), \tag{26c}$$

$$q_3^{2+}\to\sqrt{\frac{\beta(z)}{\gamma(z)}}\frac{\chi e^{\phi}(1+\kappa_4 e^{\theta_2+\theta_2^*})}{1+\tau_4 e^{\theta_2+\theta_2^*}},\quad (\theta_2+\theta_2^*\sim 0,\ \theta_1+\theta_1^*\to-\infty), \tag{26d}$$

with q_j^{1+}'s and q_j^{2+}'s ($j=1, 2, 3$) as the asymptotic expressions for the vector two solitons after the collision, respectively.

Hereby, we set Δ_j^{1-} (Δ_j^{1+}) and Δ_j^{2-} (Δ_j^{2+}) ($j=1, 2, 3$) as the amplitudes of the vector two solitons before (after) the collision. After some calculations, we obtain

$$\Delta_j^{1-}=\Delta_j^{1+}\ \text{and}\ \Delta_j^{2-}=\Delta_j^{2+},\ j=1,\ 2,\ 3, \tag{27}$$

with the condition

$$\frac{a_1^{(1)}}{a_1^{(2)}}=\frac{a_2^{(1)}}{a_2^{(2)}}=c, \tag{28}$$

where c is a nonzero constant. When $a_1^{(j)}$ and $a_2^{(j)}$ ($j=1, 2$) do not satisfy Condition (28), we have

$$\Delta_j^{1-}\neq\Delta_j^{1+}\ \text{and}\ \Delta_j^{2-}\neq\Delta_j^{2+}, \tag{29a}$$

$$\Delta_3^{1-}=\Delta_3^{1+}\ \text{and}\ \Delta_3^{2-}=\Delta_3^{2+}. \tag{29b}$$

From the asymptotic analysis earlier, we find that the appearance of the elastic or inelastic collision for the 2-bright-1-dark vector two solitons depends on the relation between $\frac{a_1^{(1)}}{a_1^{(2)}}$ and $\frac{a_2^{(1)}}{a_2^{(2)}}$. For the two bright solitons, elastic collision just occurs under Condition (28), while inelastic collision arises without Condition (28). However, collision for the dark solitons is always elastic.

Figures 7–10 show the collisions for the 2-bright-1-dark vector two solitons with the different velocities. In Figures 7 and 8, the choices of $a_1^{(1)}$ and $a_2^{(2)}$ satisfy Condition (28). In the homogeneous optical fibre where $\beta(z)$ and $\gamma(z)$ being the constants, such as $\beta(z)=\gamma(z)=4$, for the elastic collisions, amplitude and velocity for each soliton do not change before and after the collision except for a phase shift, as shown in Figure 7. For the inhomogeneous optical fibre, although the values of $\beta(z)$ and $\gamma(z)$ are variable in Figure 8, the value of $\frac{\beta(z)}{\gamma(z)}$ is a constant and the collisions are still elastic. Without Condition (28), inelastic collisions for the bright solitons occur in Figures 9a, b, d, e and 10a, b, d, e: After the collision, amplitudes of the solitons in the component q_1 increase, but they decrease in q_2. However, collisions for the dark solitons shown in Figures 9c, f and 10c, f are all elastic. Owing to the choices of $\beta(z)$ and $\gamma(z)$, the soliton velocities are invariable in Figure 9 but variable in Figure 10 during the propagation. One of the velocities of the vector two solitons shown in Figure 10 slowly decreases and eventually approaches

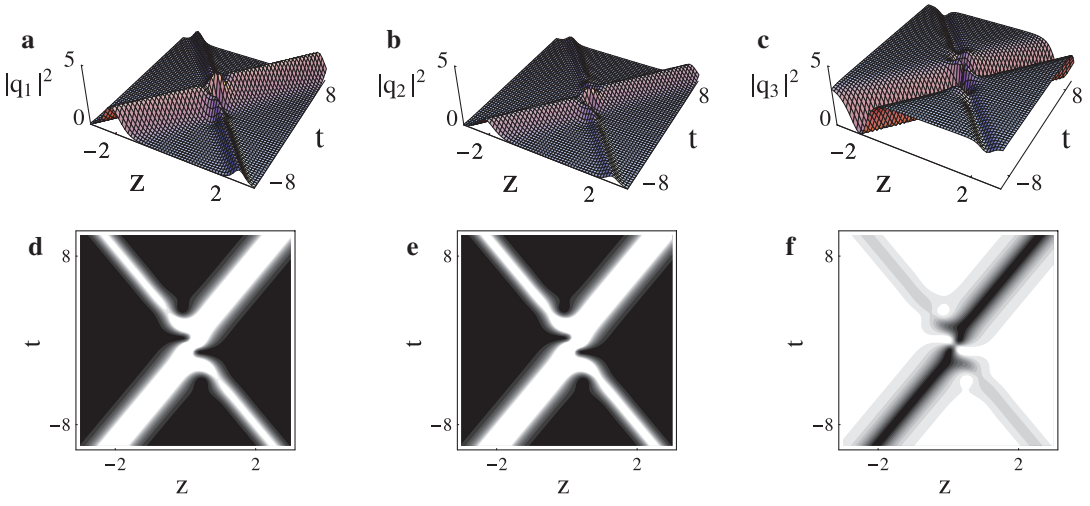

Figure 7: (a–c) Three-dimensional graphs of the elastic collision between the vector two solitons via Solutions (19) with $a_1^{(1)}=4$, $a_2^{(1)}=2$, $a_1^{(2)}=3$, $a_2^{(2)}=1.5$, $\chi=1.5+i$, $p=1$, $\eta_1=0.6+i$, $\eta_2=-1-i$, $\beta(z)=\gamma(z)=4$. (d–f) Contour plots of (a–c), respectively.

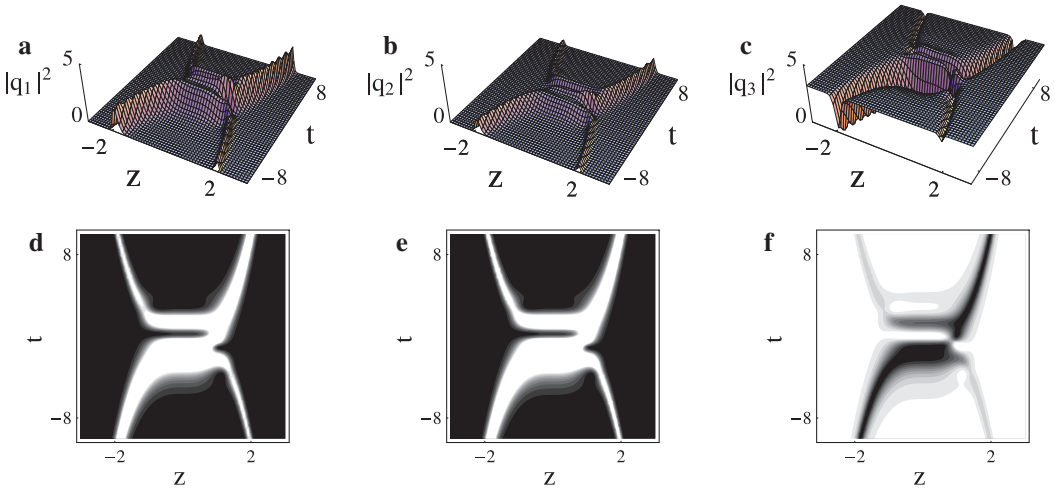

Figure 8: The same as Figure 7 except that $\beta(z)=\gamma(z)=4z^2$.

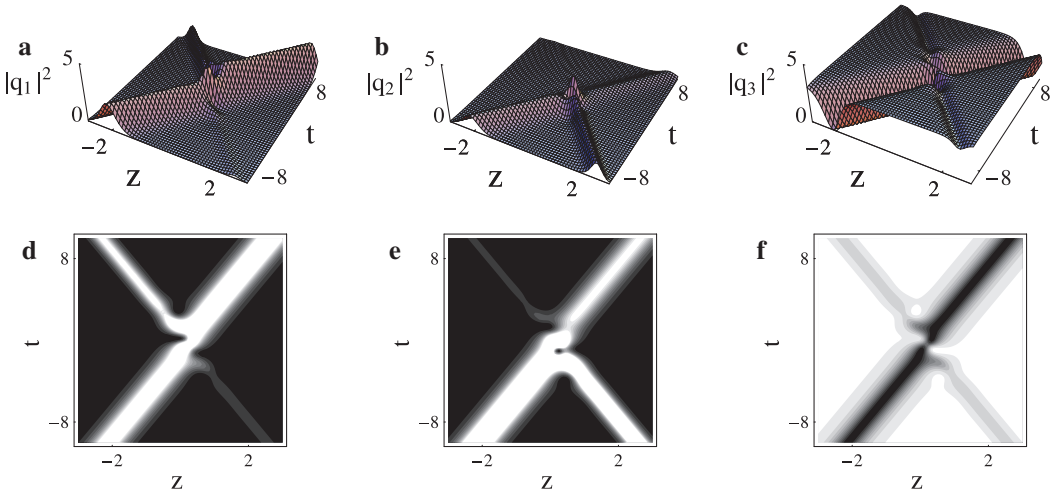

Figure 9: (a) and (b) Three-dimensional graphs of the inelastic collisions between the two bright solitons via Solutions (19). (c) Three-dimensional graph of the elastic collision between the two dark solitons via Solution (19). (d–f) Contour plots of (a–c), respectively. Hereby, the parameters are the same as those in Figure 7 except that $a_1^{(1)}=5$, $a_2^{(1)}=1.2$, $a_2^{(1)}=2$, $a_2^{(2)}=3$.

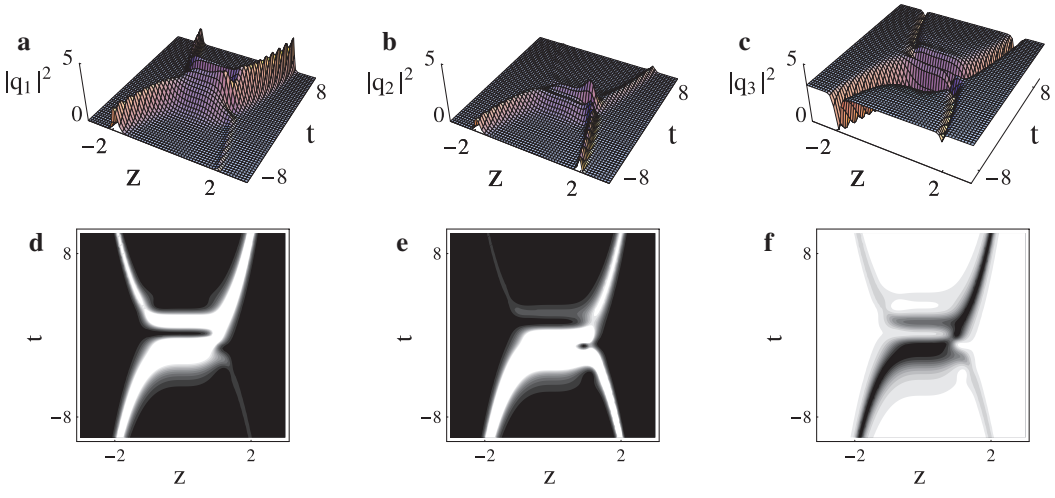

Figure 10: The same as Figure 9 except $\beta(z)=4z^2$, $\gamma(z)=4z^2$.

a steady positive velocity, while the another one slowly increases and eventually approaches a steady negative velocity for $t \to +\infty$ or $-\infty$.

(B) Asymptotic analysis on Solutions (22)

Before the collision ($z \to -\infty$),

$$q_1^{1-} \to \sqrt{\frac{\beta(z)}{\gamma(z)}} \frac{a_1 e^{\Theta_1}}{1+\sigma_1 e^{\Theta_1+\Theta_1^*}}, \quad (\Theta_1+\Theta_1^* \sim 0,\ \Theta_2+\Theta_2^* \to -\infty), \tag{30a}$$

$$q_j^{1-} \to \sqrt{\frac{\beta(z)}{\gamma(z)}} \frac{\chi_j e^{\phi_j}[1+\kappa_1^{(j)} e^{\Theta_1+\Theta_1^*}]}{1+\sigma_1 e^{\Theta_1+\Theta_1^*}} (j=2,\ 3),\ (\Theta_1+\Theta_1^* \sim 0,\ \Theta_2+\Theta_2^* \to -\infty), \tag{30b}$$

$$q_1^{2-} \to \sqrt{\frac{\beta(z)}{\gamma(z)}} \frac{A_1 e^{\Theta_2}}{\sigma_1+\nu e^{\Theta_2+\Theta_2^*}}, \quad (\Theta_2+\Theta_2^* \sim 0,\ \Theta_1+\Theta_1^* \to +\infty), \tag{30c}$$

$$q_j^{2-} \to \sqrt{\frac{\beta(z)}{\gamma(z)}} \frac{\chi_j e^{\phi_j}[\kappa_1^{(j)}+\zeta^{(j)} e^{\Theta_2+\Theta_2^*}]}{\sigma_1+\nu e^{\Theta_2+\Theta_2^*}} (j=2,\ 3),\ (\Theta_2+\Theta_2^* \sim 0,\ \Theta_1+\Theta_1^* \to +\infty), \tag{30d}$$

After the collision ($z \to +\infty$),

$$q_1^{1+} \to \sqrt{\frac{\beta(z)}{\gamma(z)}} \frac{A_2 e^{\Theta_1}}{\sigma_4+\nu e^{\Theta_1+\Theta_1^*}}, \ (\Theta_1+\Theta_1^* \sim 0,\ \Theta_2+\Theta_2^* \to +\infty), \tag{31a}$$

$$q_j^{1+} \to \sqrt{\frac{\beta(z)}{\gamma(z)}} \frac{\chi_j e^{\phi_j}[\kappa_4^{(j)}+\varsigma^{(j)} e^{\Theta_1+\Theta_1^*}]}{\sigma_4+\nu e^{\Theta_1+\Theta_1^*}} (j=2,\ 3),\ (\Theta_1+\Theta_1^* \sim 0,\ \Theta_2+\Theta_2^* \to +\infty), \tag{31b}$$

$$q_1^{2+} \to \sqrt{\frac{\beta(z)}{\gamma(z)}} \frac{a_2 e^{\theta_2}}{1+\sigma_4 e^{\Theta_2+\Theta_2^*}}, \quad (\Theta_2+\Theta_2^* \sim 0,\ \Theta_1+\Theta_1^* \to -\infty), \tag{31c}$$

$$q_j^{2+} \to \sqrt{\frac{\beta(z)}{\gamma(z)}} \frac{\chi_j e^{\phi_j}[1+\kappa_4^{(j)} e^{\Theta_2+\Theta_2^*}]}{1+\sigma_4 e^{\Theta_2+\Theta_2^*}} (j=2,\ 3),\ (\Theta_2+\Theta_2^* \sim 0,\ \Theta_1+\Theta_1^* \to -\infty), \tag{31d}$$

We set $\tilde{\Delta}_j^{1-}$ ($\tilde{\Delta}_j^{1+}$) and $\tilde{\Delta}_j^{2-}$ ($\tilde{\Delta}_j^{2+}$) (j=1, 2, 3) as the amplitudes of the vector two solitons before (after) the collision. After some calculations, we have

$$\tilde{\Delta}_j^{1-} = \tilde{\Delta}_j^{1+} \text{ and } \tilde{\Delta}_j^{2-} = \tilde{\Delta}_j^{2+}. \tag{32}$$

From Expression (32), we find that the collision for the 1-bright-2-dark vector two solitons is always elastic.

Figures 11 and 12 show the elastic collisions between the 1-bright-2-dark vector two solitons with the different velocities, for the homogeneous and inhomogeneous fibres, respectively. With $\beta(z)$ and $\gamma(z)$ being the constants, elastic collisions are shown in Figure 11. When the values of $\beta(z)$ and $\gamma(z)$ are variable and $\frac{\beta(z)}{\gamma(z)}$ is a constant, Figure 12 illustrates the different elastic collisions, where the soliton velocities are variable, and shows the same changing tendencies as those shown in Figure 10.

4.2.2 Bound States

In this part, taking the collisions between the 2-bright-1-dark vector two solitons as an example, we will investigate the effects of the GVD coefficient, $\beta(z)$, and

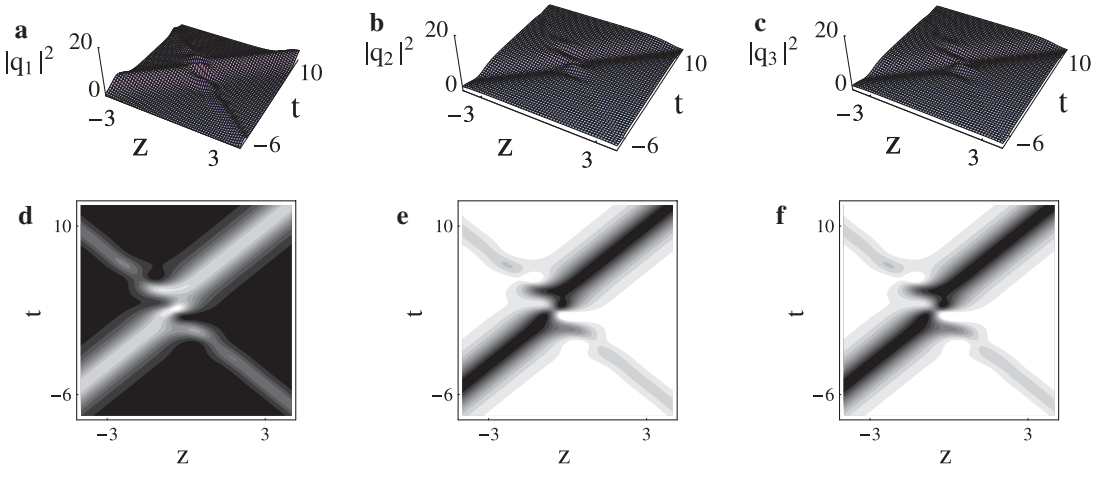

Figure 11: (a–c) Three-dimensional graphs of the elastic collision between the vector two solitons via Solutions (22) with $a_1=a_2=1$, $\chi_2=1+i$, $\chi_3=1-i$, $p_2=p_3=1$, $\mu_1=0.5+i$, $\mu_2=1-i$, $\beta(z)=\gamma(z)=2$. (d–f) Contour plots of (a–c), respectively.

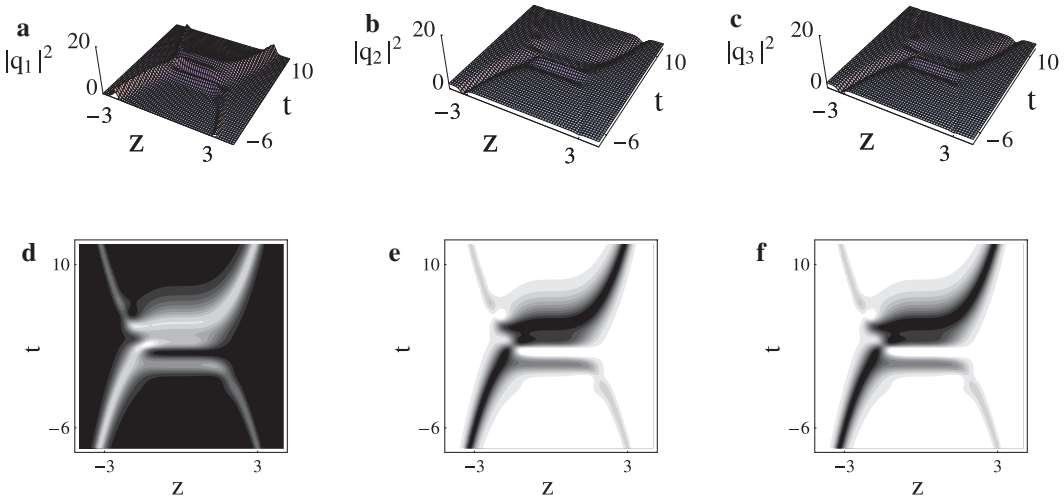

Figure 12: The same as Figure 11 except that $\beta(z)=\gamma(z)=z^2$.

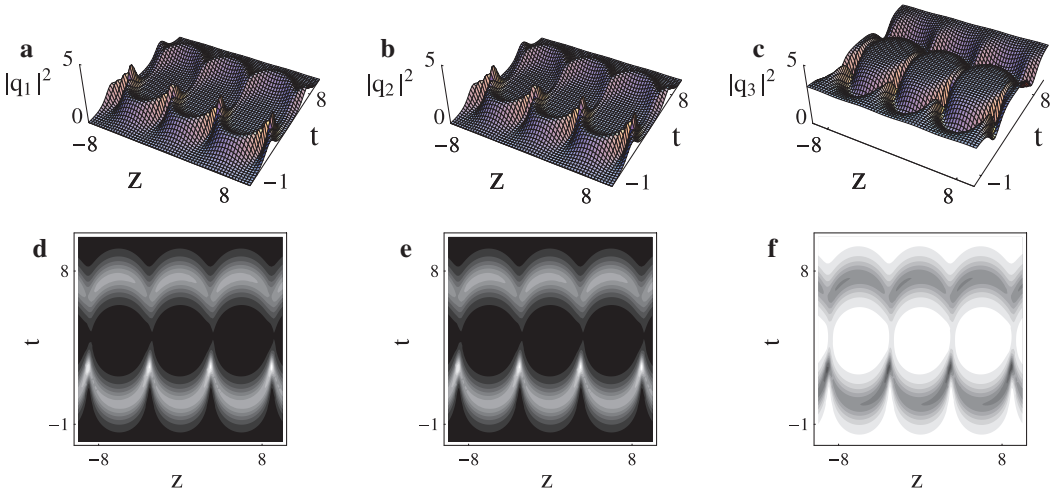

Figure 13: (a–c) Three-dimensional graphs of the bound states via Solutions (19) with $a_1^{(1)}=a_2^{(1)}=a_1^{(2)}=a_2^{(2)}=1$, $\chi=1.5+i$, $p=1$, $\eta_1=1$, $\eta_2=1.1$, $\beta(z)=\gamma(z)=10$. (d–f) Contour plots of (a–c), respectively.

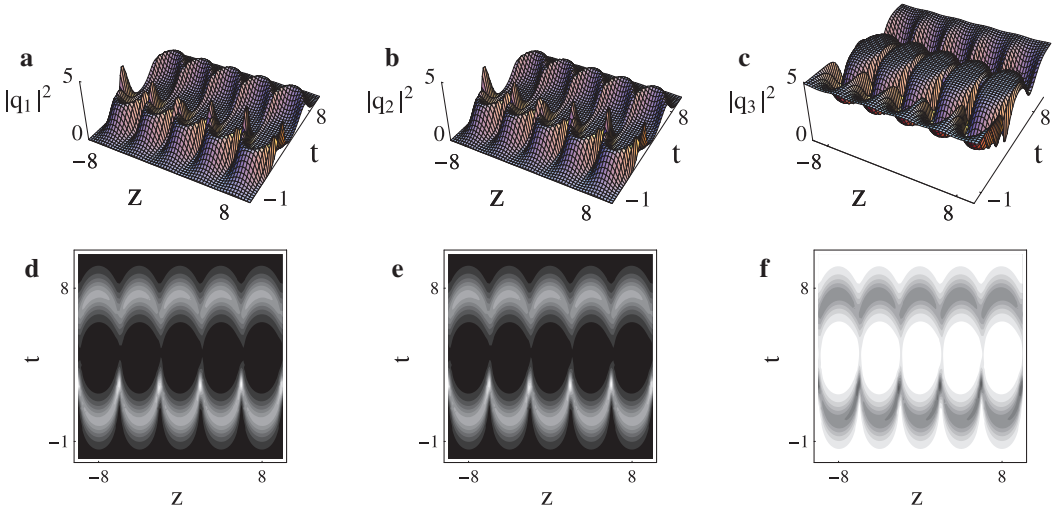

Figure 14: The same as Figure 13 except that $\beta(z)=15$.

nonlinearity coefficient, $\gamma(z)$, on the evolutions of the bound states via the graphic analysis. For the collisions between the 1-bright-2-dark vector two solitons, the analysis is similar.

Figures 13–17 show the 2-bright-1-dark vector two solitons in bound states with the invariable amplitudes, where the bound states shown in Figures 13–15 form in the homogeneous fibre, while those shown in Figures 16 and 17, in the inhomogeneous fibre. In Figures 13–15, two solitons in the components q_1, q_2, and q_3 all attract and repel each other periodically, where the values of $\beta(z)$ and $\gamma(z)$ are both constants. With the increase in $\beta(z)$, the collision period of the solitons in Figure 14 is shorter than that in Figure 13. Comparing Figures 13 and 15, we find that the collision period is independent of $\gamma(z)$. With the choices of nonconstant parameters $\beta(z)$ and $\gamma(z)$, the bound states shown in Figures 16 and 17 are different from those shown in Figures 13–15. In Figure 16, steady transmission for the vector two solitons can be achieved in a short distance at first, and then, soliton collision occurs periodically with a collision period becoming shorter and shorter. Figure 17 shows the vector two solitons attract and repel each other periodically except that the steady transmission occurs around $z=0$.

5 Conclusions

In this article, we have investigated the propagation and collision of the vector solitons from the 3-coupled variable-coefficient NLS equations, i.e. (1), which describe the amplification or attenuation of the picosecond pulses in

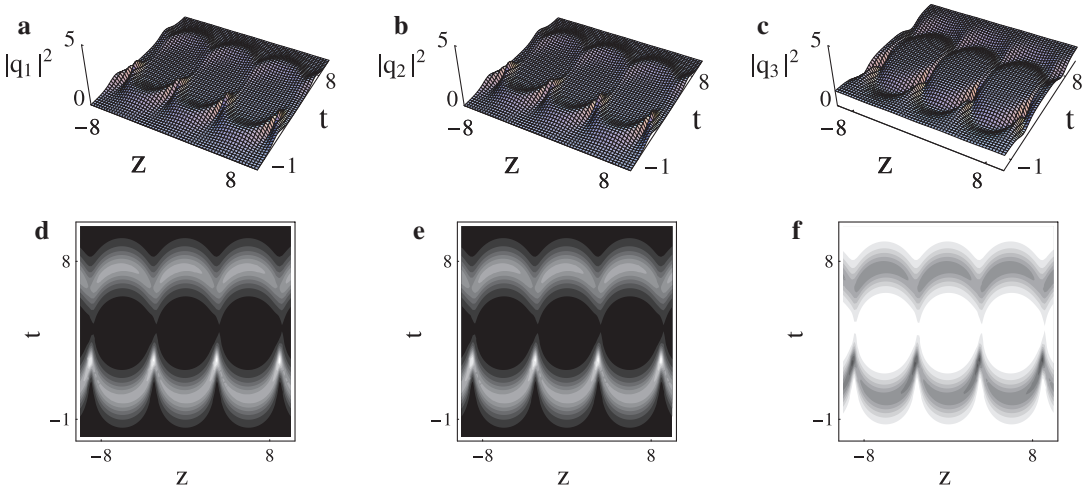

Figure 15: The same as Figure 13 except that $\gamma(z)=25$.

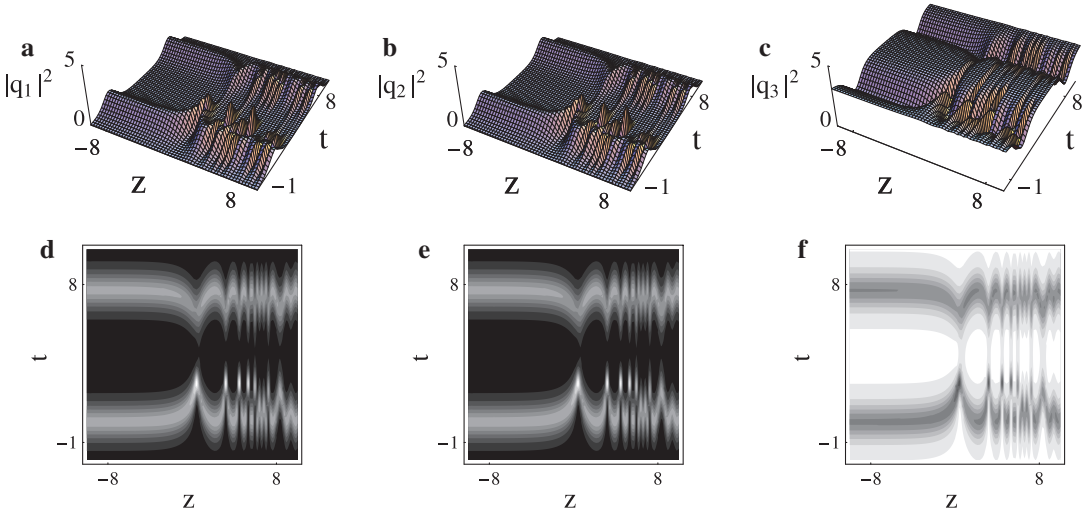

Figure 16: The same as Figure 13 except that $\beta(z)=\gamma(z)=10e^{0.4z}$.

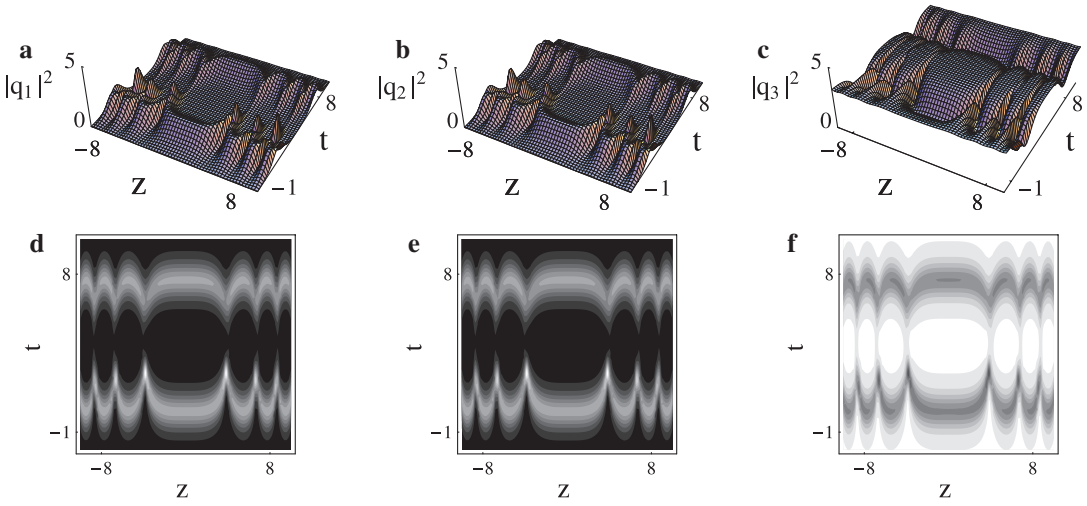

Figure 17: The same as Figure 13 except that $\beta(z)=\gamma(z)=4z$.

the inhomogeneous multicomponent optical fibre with different frequencies or polarizations. On the basis of Lax Pair (3), Infinitely-Many Conservation Laws (8) have been derived. Under Constraint (2) among the variable coefficients for the GVD, $\beta(z)$, nonlinearity, $\gamma(z)$, and fibre gain/loss, $\delta(z)$, Bilinear Forms (16), two types of the analytic mixed-type (2-bright-1-dark and 1-bright-2-dark) vector one- and two-soliton solutions, i.e. Solutions (18), (19), (21), and (22), have been obtained via the Hirota method and symbolic computation. On the basis of those solutions, influence of $\beta(z)$ and $\gamma(z)$ on the soliton propagation and collision has been analysed. With the asymptotic and graphic analysis, elastic and inelastic collisions between the vector two solitons have been studied. We have also analysed the effects of $\beta(z)$ and $\gamma(z)$ on the bound states via the graphic analysis. Attention should be paid to the following aspects:

1. Amplitudes of the bright and dark solitons are both related to $\beta(z)$ and $\gamma(z)$, while their velocities are only related to $\beta(z)$.
2. With the choices of $\beta(z)$ and $\gamma(z)$, the vector soliton propagates in different forms, as seen in Figures 1, 2, 4, and 5. Besides, amplitude-changing optical vector soliton can be obtained when the value of $\frac{\beta(z)}{\gamma(z)}$ is variable, as seen in Figures 3 and 6.
3. For the 2-bright-1-dark vector two solitons, elastic collision for the two bright solitons only occurs with Condition (28), as seen in Figures 7a, b, d, e and 8a, b, d, e, whereas inelastic collision arises without Condition (28), as seen in Figures 9a, b, d, e and 10a, b, d, e. Collision for the dark solitons is always elastic, as seen in Figures 7c, f, 8c, f, 9c, f and 10c, f.
4. For the 1-bright-2-dark vector two solitons, collision in each component is elastic, as seen in Figures 11 and 12.
5. For the bound states, $\beta(z)$ and $\gamma(z)$ affect their types, as seen in Figures 13–17. Besides, with $\beta(z)$ and $\gamma(z)$ being the constants, collision period decreases as $\beta(z)$ increases but is independent of $\gamma(z)$, as seen in Figures 13–15.

Acknowledgments: We express our sincere thanks to the Editors and Reviewers for their valuable comments. This work has been supported by the National Natural Science Foundation of China under Grant Nos. 11272023 and 11471050, by the Fund of State Key Laboratory of Information Photonics and Optical Communications (Beijing University of Posts and Telecommunications), and by the Fundamental Research Funds for the Central Universities of China under Grant No. 2011BUPTYB02.

References

[1] P. D. Green and A. Biswas, Commun. Nonlinear Sci. Numer. Simul. **15**, 3865 (2010).
[2] A. Biswas and D. Milovic, Commun. Nonlinear Sci. Numer. Simul. **15**, 1473 (2010).
[3] A. Hasegawa and F. Tappert, Appl. Phys. Lett. **23**, 142 (1973).
[4] L. F. Mollenauer, R. H. Stolen, and J. P. Gordon, Phys. Rev. Lett. **45**, 1095 (1980).
[5] M. S. Mani Rajana, A. Mahalingamb, and A. Uthayakumarc, Ann. Phys. **346**, 1 (2014).
[6] C. Q. Su, Y. T. Gao, L. Xue, and X. Yu, Z. Naturforsch. A **70**, 935 (2015).
[7] T. Kanna and M. Lakshmanan, Phys. Rev. Lett. **86**, 5043 (2001).

[8] Q. M. Wang, Y. T. Gao, C. Q. Su, Y. J. Shen, Y. J. Feng, et al., Z. Naturforsch. A **70**, 365 (2015).
[9] H. Nakatsuka, D. Grischkowsky, and A. C. Balant, Phys. Rev. Lett. **47**, 910 (1981).
[10] H. Bulut, Y. Pandir, and S. Tuluce Demiray, Waves Random Complex Media **24**, 439 (2014).
[11] G. P. Agrawal, Nonlinear Fiber Optics, Academic Press, New York 1995.
[12] C. R. Menyuk, Opt. Lett. **12**, 614 (1987).
[13] C. R. Menyuk, J. Opt. Soc. Am. B **5**, 392 (1988).
[14] R. Radhakrishnan, P. T. Dinda, and G. Millot, Phys. Rev. E **69**, 046607 (2004).
[15] R. Radhakrishnan, M. Lakshmanan, and J. Hietarinta, Phys. Rev. E **56**, 2213 (1997).
[16] R. Radhakrishnan and K. Aravinthan, J. Phys. A **40**, 13023 (2007).
[17] A. P. Sheppard and Y. S. Kivshar, Phys. Rev. E **55**, 4473 (1997).
[18] X. Lü, J. Li, H. Q. Zhang, T. Xu, L. L. Li, et al. J. Math. Phys. **51**, 043511 (2010).
[19] W. R. Shan, F. H. Qi, R. Guo, Y. S. Xue, P. Wang, et al. Phys. Scr. **85**, 015002 (2012).
[20] J. W. Yang, Y. T. Gao, Q. M. Wang, C. Q. Su, Y. J. Feng, et al., Physica B **481**, 148 (2016).
[21] M. Hisakado and M. Wadati, J. Phys. Soc. Jpn. **64**, 408 (1995).
[22] M. Hisakado, T. Iizuka, and M. Wadati, J. Phys. Soc. Jpn. **63**, 2887 (1994).
[23] Y. J. Feng, Y. T. Gao, Z. Y. Sun, D. W. Zuo, Y. J. Shen, et al., Phys. Scr. **90**, 045201 (2015).
[24] Q. M. Wang, Y. T. Gao, C. Q. Su, B. Q. Mao, Z. Gao, et al., Ann. Phys. **363**, 440 (2015).
[25] C. Q. Dai and H. P. Zhu, Ann. Phys. **341**, 142 (2014).
[26] V. I. Kruglov, A. C. Peacock, and J. D. Harvey, Phys. Rev. E **71**, 056619 (2005).
[27] S. Kumar, K. Singh, and R. K. Gupta, Commun. Nonlinear Sci. Numer. Simul. **17**, 1529 (2012).
[28] F. H. Qi, H. M. Ju, X. H. Meng, and J. Li, Nonlinear Dyn. **77**, 1331 (2014).
[29] X. W. Zhou and L. Wang, Comput. Math. Appl. **61**, 2035 (2011).
[30] H. J. Li, J. P. Tian, and L. J. Song, Optik **124**, 7040 (2013).
[31] J. Tian and G. Zhou, Eur. Phys. J. D **41**, 171 (2007).
[32] V. R. Kumar, R. Radha, and K. Porsezian, Eur. Phys. J. D **57**, 387 (2010).
[33] R. Hirota, J. Math. Phys. **14**, 805 (1973).
[34] R. Hirota, The Direct Method in Soliton Theory, Cambridge University Press, Cambridge 2004.
[35] B. Tian and Y. T. Gao, Phys. Lett. A **362**, 283 (2007).
[36] C. Q. Su, Y. T Gao, X. Yu, L. Xue, and Y. J. Shen, J. Math. Anal. Appl. **435**, 735 (2016).
[37] P. Jin, C. A. Bouman, and K. D. Sauer, IEEE Trans. Comput. Imaging **1**, 200 (2015).
[38] K. Konno, H. Sanuki, and Y. H. Ichikawa, Prog. Theor. Phys. **52**, 886 (1974).
[39] H. Sanuki and K. Konno, Phys. Lett. A **48**, 221 (1974).